Inorg. Chem. **2003**, *42*, 7200–7206

Tropochemical Cell-Twinning in the New Quaternary Bismuth Selenides $K_xSn_{6-2x}Bi_{2+x}Se_9$ and $KSn_5Bi_5Se_{13}$

Antje Mrotzek and Mercouri G. Kanatzidis*

Department of Chemistry and Center for Fundamental Materials Research, Michigan State University, East Lansing, Michigan 48824

Received March 8, 2003

The quaternary $K_xSn_{6-2x}Bi_{2+x}Se_9$ and $KSn_5Bi_5Se_{13}$ were discovered from reactions involving K_2Se, Bi_2Se_3, Sn, and Se. The single crystal structures reveal that $K_xSn_{6-2x}Bi_{2+x}Se_9$ is isostructural to the mineral heyrovskyite, $Pb_6Bi_2S_9$, crystallizing in the space group *Cmcm* with $a = 4.2096(4)$ Å, $b = 14.006(1)$ Å, and $c = 32.451(3)$ Å while $KSn_5Bi_5Se_{13}$ adopts a novel monoclinic structure type (*C*2/*m*, $a = 13.879(4)$ Å, $b = 4.205(1)$ Å, $c = 23.363(6)$ Å, $\beta = 99.012(4)°$). These compounds formally belong to the lillianite homologous series $xPbS\cdot Bi_2S_3$, whose characteristic is derivation of the structure by tropochemical cell-twinning on the (311) plane of the NaCl-type lattice with a mirror as twin operation. The structures of $K_xSn_{6-2x}Bi_{2+x}Se_9$ and $KSn_5Bi_5Se_{13}$ differ in the width of the NaCl-type slabs that form the three-dimensional arrangement. While cell-twinning of 7 octahedra wide slabs results in the heyrovskyite structure, 4 and 5 octahedra wide slabs alternate in the structure of $KSn_5Bi_5Se_{13}$. In both structures, the Bi and Sn atoms are extensively disordered over the metal sites. Some physicochemical properties of $K_xSn_{6-2x}Bi_{2+x}Se_9$ and $KSn_5Bi_5Se_{13}$ are reported.

Introduction

There is a strong interest in developing new physicochemical concepts in designing materials with superior thermoelectric properties[1–3] Our approach, which has been outlined in detail elsewhere,[4] is focused on complex quaternary and ternary bismuth chalcogenides with a derivatized Bi_2Te_3-type framework through the incorporation of alkali metals. The examples of $CsBi_4Te_6$[5] and β $-K_2Bi_8Se_{13}$[6,7] show that these exploratory investigations can lead to novel thermoelectric materials with promising properties. Therefore, we expanded our investigations to quaternary systems to further explore the effects of structural complexity and mass fluctuation on the physical properties. In this context, we recently described the quaternary selenides, $A_{1-x}M_{3-x}Bi_{11+x}Se_{20}$,[8] $A_{1-x}M_{4-x}Bi_{11+x}Se_{21}$,[9] $K_{1-x}Sn_{5-x}Bi_{11+x}Se_{22}$,[10]

* To whom correspondence should be addressed. E-mail: kanatzid@cem.msu.edu.

(1) (a) Slack, G. A. In *CRC Handbook of Thermoelectrics*; Rowe, D. M., Ed.; CRC Press: Boca Raton, FL, 1995; pp 407−440. (b) Slack, G. A. In *Solid State Physics*; Ehrenreich, H., Seitz, F., Turnbull, D., Eds.; Academic: New York, 1997; Vol. 34, p 1. (c) Sales, B. C. *Mater. Res. Bull.* **1998**, *23*, 15−21. (d) Sales, B. C.; Mandrus, D.; Chakoumakos, B. C.; Keppens, V.; Thompson, J. R. *Phys. Rev. B.* **1997**, *56*, 15081−15089. (e) Tritt, T. M. *Science* **1996**, *272*, 1276−1277.

(2) See papers in this volume: *Thermoelectric Materials 2000—The Next Generation Materials for Small-Scale Refrigeration and Power Applications*; Tritt, T. M., Nolas, G. S., Mahan, G. D., Mandrus, D., Kanatzidis, M. G., Eds.; Materials Research Society Symposium Proceedings 626; Elsevier: New York, 2000.

(3) (a) *CRC Handbook of Thermoelectrics*; Rowe, D. M., Ed.; CRC Press: Boca Raton, FL, 1995. (b) Hicks, L. D.; Dresselhaus, M. S. *Phys. Rev. B* **1993**, *47*, 12727−12731. (c) Hicks, L. D.; Dresselhaus, M. S. *Phys. Rev. B* **1993**, *47*, 16631−16634. (d) Hicks, L. D.; Harmann, T. C.; Dresselhaus, M. S. *Appl. Phys. Lett.* **1993**, *63*, 3230−3232. (e) Broido, D. A.; Reinecke, T. L. *Appl. Phys. Lett.* **1995**, *67*, 1170−1171. (f) Sofo, J. O.; Mahan, G. D. *Appl. Phys. Lett.* **1994**, *65*, 2690−2692.

(4) (a) Kanatzidis, M. G.; DiSalvo, F. J. *ONR Quarterly Reviews* **1996**, *XXVII*, 14−22. (b) Chung, D.-Y.; Iordanidis, L.; Choi, K.-S.; Kanatzidis, M. G. *Bull. Korean Chem. Soc.* **1998**, *19*, 1283−1293. (c) Kanatzidis, M. G. *Semicond. Semimet.* **2001**, *69*, 51−100.

(5) Chung, D.-Y.; Hogan, T.; Brazis, P. W.; Rocci-Lane, M.; Kannewurf, C. R.; Bastea, M.; Uher, C.; Kanatzidis, M. G. *Science* **2000**, *287*, 1024−1027.

(6) (a) Kanatzidis, M. G.; Chung, D.-Y.; Iordanidis, L.; Choi, K.-S.; Brazis, P.; Rocci, M.; Hogan, T.; Kannewurf, C. *Mater. Res. Soc. Symp. Proc.* **1998**, *545*, 233−246. (b) Bravis, P. W.; Rocci-Lane, M. A.; Ireland, J. R.; Chung, D.-Y.; Kanatzidis, M. G.; Kannewurf, C. R. Proceedings of the XVIIIth International Conference On Thermoelectrics (ITC '99); Baltimore, MD, 1999; p 619−622.

(7) (a) Kanatzidis, M. G.; McCarthy, T. J.; Tanzer, T. A.; Chen, L.-H.; Iordanidis, L.; Hogan, T.; Kannewurf, C. R.; Uher, C.; Chen, B. *Chem. Mater.* **1996**, *8*, 1465−1474. (b) Chen, B.; Uher, C.; Iordanidis, L.; Kanatzidis, M. G. *Chem. Mater.* **1997**, *9*, 1655−1658.

(8) Mrotzek, A.; Iordanidis, L.; Kanatzidis, M. G. *Inorg. Chem.* **2001**, *40*, 6204−6211.

(9) Mrotzek, A.; Chung, D.-Y.; Ghelani, N.; Hogan, T.; Kanatzidis, M. G. *Chem. Eur. J.* **2001**, *7*, 1915−1926.

(10) (a) Mrotzek, A.; Chung, D.-Y.; Hogan, T.; Kanatzidis, M. G. *J. Mater. Chem.* **2000**, *10*, 1667−1672. (b) Mrotzek, A.; Kanatzidis, M. G. *J. Solid State Chem.* **2002**, *167*, 299−301.

10.1021/ic034252n CCC: $25.00
Published on Web 10/08/2003

$A_{1+x}M_{3-2x}Bi_{7+x}Se_{14}$,[8] $K_{1+x}Sn_{4-2x}Bi_{7+x}Se_{15}$,[11] and $A_{1-x}Sn_{9-x}Bi_{11+x}Se_{26}$[12] with A = K, Rb, Cs and M = Sn, Pb. They all belong to the homologous series $A_m[M_{1+l}Se_{2+l}]_{2m}[M_{2l+n}Se_{2+3l+n}]$ with $l = 2$.[13] The term homologous series characterizes a chemical series of phases that are expressed by general formulas and built on common structural principles. Besides oxides,[14] homologous series are also known among sulfosalts, as for example the lillianite homologous series,[15,16] xPbSBi_2S_3, which is found for minerals in the PbS−Bi_2S_3[16] and Ag_2S−PbS−Bi_2S_3[16c,17] system. Its members are generated by tropochemical cell-twinning[18,19] of galena slabs (NaCl-type) cut perpendicular to the (311) direction with a mirror as twinning operation. Tropochemical cell twinning is a twinning on the cell scale which is reported for minerals. This phenomenon is found for structural changes accompanied by a change in chemical composition. Also, it can be seen as a stress-relieving mechanism to accommodate impurities in the crystal. Figure 1 depicts this tropochemical cell-twinning on (311) of a NaCl-type block where the continuation of the original galena lattice is indicated by light gray drawing. The different homologues of the lillianite series vary in the thickness of the NaCl-type blocks. The various members are identified by the number of metal octahedra along the (111) direction of the galena slabs. Therefore, the mineral lillianite, $Pb_3Bi_2S_6$,[15] is also addressed as L 4,4, which indicates that two identical, 4 octahedra wide blocks undergo the cell-twinning. Structures composed of two distinct blocks are also known, as for example vikingite,[20] $Ag_4Pb_{10}Bi_{12}S_{30}$, with 4 and 7 metal octahedra wide slabs. In contrast to those homologies, the $A_m[M_{1+l}Se_{2+l}]_{2m}[M_{2l+n}Se_{2+3l+n}]$ series is characterized by three independent integers *l*, *m*, and *n* which cause structural evolution in three different dimensions. The series has predictive character, and charge-balanced, hypothetical members can be easily generated according to the general formula. In the process of exploring the limits of this grand series, we investigated also the Sn rich area (large *m* values) of the quaternary system K/Sn/Bi/Se which led to two new quaternary phases that turned out to belong to a different series, namely the extended lillianite family. We report the crystal structure and physicochemical properties of $K_xSn_{6-2x}Bi_{2+x}Se_9$ and $KSn_5Bi_5Se_{13}$, and we discuss their relationship to the known members of the lillianite series.

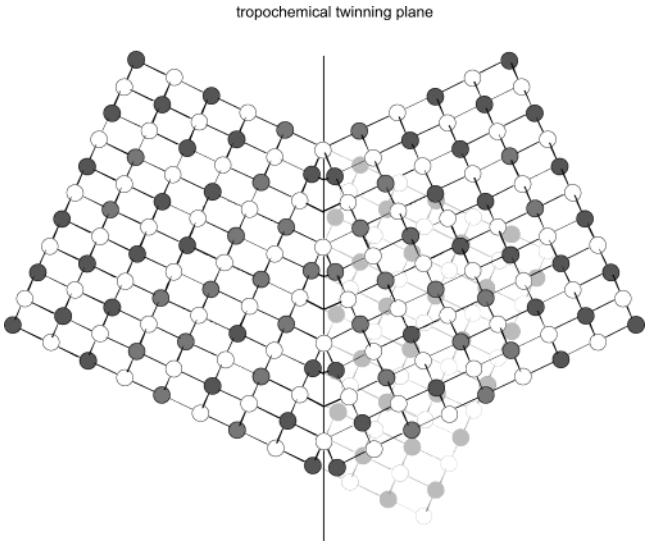

Figure 1. Tropochemical twinning on (311) of NaCl-type blocks with mirror as twin operation. Light gray indicates the continuation of the original galena lattice.

Experimental Section

Synthesis. All manipulations were carried out under a dry nitrogen atmosphere in a Vacuum Atmospheres Dri-Lab glovebox. The starting material Bi_2Se_3 was obtained by reaction of stoichiometric amounts of the elements (99.999% purity) in evacuated quartz glass ampules at 800 °C for 3 days. The K_2Se was prepared by stoichiometric reaction of potassium metal and selenium in liquid ammonia.

$K_xSn_{6-2x}Bi_{2+x}Se_9$. A mixture of K_2Se (1 mmol), Sn (8 mmol), Se (8 mmol), and Bi_2Se_3 (3 mmol) was loaded in a carbon-coated quartz tube (9 mm diameter) and sealed at a residual pressure of $< 10^{-4}$ Torr. The starting materials were heated within 24 h to 800 °C and kept there for 24 h, followed by slow cooling to 50 °C at a rate of 0.5 °C/min. A silver-gray polycrystalline ingot of $K_xSn_{6-2x}Bi_{2+x}Se_9$ was obtained. A quantitative microprobe analysis with a SEM/EDS system performed on different crystals gave the following average composition $K_{0.4}Sn_{4.3}Bi_{2.7}Se_9$.

$KSn_5Bi_5Se_{13}$. A mixture of K_2Se (1 mmol), Sn (10 mmol), Se (10 mmol), and Bi_2Se_3 (5 mmol) was loaded in a quartz tube (9 mm diameter) and sealed at a residual pressure of $<10^{-4}$ Torr. *To prevent an explosion of the tube during the following procedure, the length of the tube was longer than usual. The tube was carefully placed under the flame of a natural gas-oxygen torch until the mixture melted, and then, the tube was removed from the flame and let to solidify. The so-called "flame reaction" has to be carried out by a cautious and experienced operator using protection shields and helmet.* A silver-gray ingot of $KSn_5Bi_5Se_{13}$ was obtained. A quantitative microprobe analysis with a SEM/EDS system performed on different crystals gave the following average composition $K_{0.7}Sn_{4.3}Bi_{5.7}Se_{13}$. A reaction procedure analogous to $K_xSn_{6-2x}Bi_{2+x}Se_9$ yields in a different phase with similar composition, $K_{1-x}Sn_{9-x}Bi_{11+x}Se_{26}$,[12] a member of the homologous series $A_m[M_{1+l}Se_{2+l}]_{2m}[M_{2l+n}Se_{2+3l+n}]$.

(11) Choi, K.-S.; Chung, D.-Y.; Mrotzek, A.; Brazis, P. W.; Kannewurf, C. R.; Uher, C.; Chen, W.; Hogan, T.; Kanatzidis, M. G. *Chem. Mater.* **2001**, *13*, 756−764.
(12) Mrotzek, A.; Kanatzidis, M. G. *Chem. Commun.* **2001**, 1648−1649.
(13) Mrotzek, A.; Kanatzidis, M. G. *Acc. Chem. Res.* **2003**, *36*, 111−119.
(14) (a) Magnéli, A. *Acta Crystallogr.* **1953**, *6*, 495. (b) Frit, B.; Mercurio, J. P. *J. Alloys Compd.* **1992**, *188*, 27−35. (c) Gopalakrishnan, J.; Sivakumar, T.; Thangadurai, V.; Subbanna, G. N. *Inorg. Chem.* **1999**, *38*, 2802.
(15) (a) Takagi, J.; Takuchi, Y.; *Acta Crystallogr.* **1972**, *B28*, 369−373. (b) Otto, H. H.; Strunz, H. *Neues Jahrb. Mineral., Abh.* **1968**, *108*, 1−19.
(16) (a) Makovicky, E.; Karup-Moeller, S. *Neues Jahrb. Mineral., Abh.* **1977**, *130*, 264−287. (b) Makovicky, E. *Neues Jahrb. Mineral., Abh.* **1977**, *131*, 187−207. (c) Makovicky, E.; Karup-Moeller, S. *Neues Jahrb. Mineral., Abh.* **1977**, *131*, 56−82. (d) Makovicky, E. *Neues Jahrb. Mineral., Abh.* **1989**, *160*, 269−297.
(17) (a) Skowron, A.; Tilley, R. J. D. *J. Solid State Chem.* **1989**, *78*, 84−92. (b) Skowron, A.; Tilley, R. J. D. *J. Solid State Chem.* **1990**, *85*, 235−250.
(18) Tropochemical is from the Greek: tropos = turn, change.
(19) (a) Takuchi, Y. *Tropo-Chemical Cell-Twinning—A Structure Building Mechanism in Crystalline Solids*; Terra Scientific Publishing Company: Tokyo, 1997. (b) Takuchi, Y. *Z. Kristallogr.* **1979**, *150*, 75−84. (c) Takuchi, Y. *Recent Prog. Nat. Sci. Jpn.* **1978**, *3*, 153−181. (d) Takuchi, Y.; Takagi, J. *Proc. Jpn. Acad.* **1974**, *50*, 843−847. (e) Anderson, S.; Hyde, B. G. *J. Solid State Chem.* **1974**, *9*, 92−101.
(20) Makovicky, E.; Mumme, W. G.; Madsen, I. C. *Neues Jahrb. Mineral., Abh.* **1992**, *10*, 454−68.

Physical Measurements. Electron Microscopy. Quantitative microprobe analyses of the compounds were performed with a JEOL JSM-35C SEM equipped with a Tracer Northern EDS detector. Data were acquired using an accelerating voltage of 25 kV and a 60 s accumulation time. The quantitative microprobe analyses have a standard deviation of about 2−5%.

Differential Thermal Analysis. Differential thermal analysis (DTA) was performed with a computer-controlled Shimadzu DTA-50 thermal analyzer as described earlier.[10] The samples were heated to 800 °C at 10 °C/min, and isothermed for 5 min followed by cooling at −10 °C/min to 50 °C.

Infrared Spectroscopy. Diffuse reflectance spectra were recorded in the region 6000−400 cm^{-1} with the use of a Nicolet MAGNA-IR 750 spectrometer equipped with a collector diffuse reflectance accessory from Spectra-Tech, Inc. Band gaps were obtained as described elsewhere.[7]

Charge Transport Measurements. Room temperature conductivity measurements were performed in the usual four-probe geometry. The Seebeck coefficient was measured between 300 and 400 K by using a SB-100 Seebeck effect measurement system, MMR Technologies, Inc.

Powder X-ray Diffraction. Powder patterns of all starting materials and products were obtained using a CPS 120 INEL X-ray powder diffractometer equipped with a position-sensitive detector and graphite monochromatized Cu Kα radiation. The purity and homogeneity was confirmed by comparing the X-ray powder diffraction pattern to that calculated from single crystal data using the CERIUS[2] software.[21]

Single Crystal X-ray Crystallography. Single crystals of $K_{0.54}Sn_{4.92}Bi_{2.54}Se_9$ and $KSn_5Bi_5Se_{13}$ were mounted on the tip of a glass fiber. The intensity data were collected on a Siemens SMART Platform CCD diffractometer with graphite monochromatized Mo Kα radiation and the SMART software[22] for data acquisition. The extraction and reduction of the data were performed with the program SAINT.[23] The systematic absences observed for $K_{054}Sn_{4.92}Bi_{2.54}Se_9$ led to the space group *Cmcm* while $KSn_5Bi_5Se_{13}$ crystallizes in *C*2/*m*. An analytical absorption correction was performed in each case followed by a semiempirical absorption correction based on symmetrically equivalent reflections with the program SADABS. The crystal structures were solved with direct methods (SHELXS-97) and refined using the SHELXTL package of crystallographic programs.

$K_{0.54}Sn_{4.92}Bi_{2.54}Se_9$. Eleven crystallographically independent positions (Bi1−4, Sn1, and Se1−6) were found situated on mirror planes ($x = 0$ and $^1/_2$). The structure refinement revealed unusually high thermal displacement parameters for the Bi1−4 sites and the Sn1 site introducing a disorder model with mixed Bi/Sn occupancies and Sn/K occupancies, respectively, in the same crystallographic site. The refinement resulted in 58% Sn in the Bi1 site, 31% Sn in the Bi2 site, 90% Sn in the Bi3 site, 64% Sn in the Bi4 site. The Sn1 site is occupied by 23% Sn and 27% K; the space group *Cmcm* creates an equivalent position only 0.5 Å apart from Sn1 setting the maximum occupancy of the Sn1 site to 50%. Assuming K^+, Sn^{2+}, Bi^{3+}, and Se^{2-}, the refinement led to the charged balanced formula $K_xSn_{6-2x}Bi_{2+x}Se_9$ which was then used to constrain the occupancies of the disordered sites. After anisotropic refinement, the R1 and wR2 values dropped to 3.5% and 6.7%, respectively.

(21) *CERIUS*[2], version 1.6; Molecular Simulations, Inc.: Cambridge, England, 1994.
(22) *SMART*; Siemens Analytical X-ray Systems Inc.: Madison, WI, 1996.
(23) *SAINT V-4*; Siemens Analytical X-ray Systems Inc.: Madison WI, 1994−196.

Table 1. Summary of Crystallographic Data and Structural Analysis

formula	$K_{0.54}Sn_{4.92}Bi_{2.54}Se_9$	$K_1Sn_5Bi_5Se_{13}$
space group	*Cmcm*	*C*2/*m*
a, Å	4.2096(4)	13.879(4)
b, Å	14.006(1)	4.205(1)
c, Å	32.451(3)	23.363(6)
β, deg	90	99.012(4)
Z; *V*, Å^3	4; 1913.2(3)	2, 1346.6(6)
D_{calcd}, g/cm^{-3}	6.428	6.668
T, K	298	298
λ(Mo Kα), Å	0.71073	0.71073
μ(Mo Kα)/cm^{-1}	49.942	54.808
final R1/wR2[a] ($I > 2\sigma$), %	3.51/6.73	7.52/14.27

[a] $R1 = \sum||F_o| - |F_c||/\sum|F_o|$, $wR2 = \{\sum[w(F_o^2 - F_c^2)^2]/\sum[w(F_o^2)^2]\}^{1/2}$.

Table 2. Fractional Atomic Coordinates and Equivalent Atomic Displacement Parameter (U_{eq}) Values in 10^{-3} Å^2 for $K_{0.54}Sn_{4.92}Bi_{2.54}Se_9$ with Estimated Standard Deviations in Parentheses

	x	*y*	*z*	sof	U_{eq}[a]
Bi1/Sn1′	0	0.1782(1)	0.3267(1)	0.419(9)/0.581	14(1)
Bi2/Sn2′	−0.5	−0.0440(1)	0.3833(1)	0.69(1)/0.31	13(1)
Bi3/Sn3′	−0.5	0.2302(1)	0.4424(1)	0.102(8)/0.898	12(1)
Bi4/Sn4′	0	0	0.5	0.36(1)/0.64	14(1)
Sn1/K1′	−0.5	0.4019(4)	0.2584(1)	0.231(8)/0.269[b]	54(2)
Se1	−0.5	0.0486(1)	0.3079(1)	1	12(1)
Se2	0	0.0920(1)	0.4171(1)	1	10(1)
Se3	−0.5	−0.1373(1)	0.4737(1)	1	10(1)
Se4	−0.5	0.3262(1)	0.3580(1)	1	17(1)
Se5	0	0.2578(1)	0.25	1	15(1)

[a] U_{eq} is defined as one-third of the trace of the orthogonalized U_{ij} tensor. [b] Maximum occupation 50%.

Table 3. Fractional Atomic Coordinates and Equivalent Atomic Displacement Parameter (U_{eq}) Values in 10^{-3} Å^2 for $K_1Sn_5Bi_5Se_{13}$ with Estimated Standard Deviations in Parentheses

	x	*y*	*z*	sof	U_{eq}[a]
Bi1/Sn1′	0.9974 (1)	0.5	0.1603(1)	0.46(1)/0.54	19(1)
Bi2/Sn2′	0.7544(1)	0	0.0829(1)	0.69(1)/0.31	21(1)
Bi3/Sn3′	0.0545(1)	0.5	0.3777(1)	0.37(1)/0.63	17(1)
Bi4/Sn4′	0.8501(1)	0	0.4557(1)	0.48(1)/0.52	14(1)
Bi5/K5′	0.2587(3)	0	0.2653(3)	0.50(1)/0.50	80(1)
Sn1	0	0	0	1	24(1)
Se1	0.8759(2)	0.5	0.0392(1)	1	17(1)
Se2	0.6312(2)	0.5	0.1217(2)	1	37(1)
Se3	0.8728(2)	0	0.1918(1)	1	21(1)
Se4	0.1171(2)	0.5	0.2692(1)	1	28(1)
Se5	0.9148(2)	0	0.3473(1)	1	23(1)
Se6	0.7117(2)	0.5	0.4173(1)	1	25(1)
Se7	0	0.5	0.5	1	19(1)

[a] U_{eq} is defined as one-third of the trace of the orthogonalized U_{ij} tensor.

The results of the structure refinements and other crystallographic data are given in Tables 1, 2, 4, and 6.

$KSn_5Bi_5Se_{13}$. Thirteen crystallographically independent positions (Bi1−5, Sn1, and Se1−7) were found situated on mirror planes ($y = 0$ and $^1/_2$). The structure refinement revealed unusually high thermal displacement parameters for the Bi1−5 sites introducing a disorder model with mixed Bi/Sn occupancies in the same crystallographic site. The refinement resulted in 54% Sn in the Bi1 site, 31% Sn in the Bi2 site, 63% Sn in the Bi3 site, 52% in the Bi4 site, and 82% Sn in the Bi5 site. A release of the occupancy of the Sn1 site led to full occupancy by Sn within standard derivation. In contrast, the EDS analyses of the bulk material (composition determined by EDS: $K_{0.7}Sn_{4.3}Bi_{5.7}Se_{13}$) and the very same crystal (composition determined by EDS: $K_{0.4}Sn_{4.0}Bi_{5.3}Se_{13}$) whose intensity data had been collected indicate that the crystal contains a significant amount of potassium. According to our experience,

Table 4. Anisotropic Displacement Parameters (10^{-3} Å^2) for $K_{0.54}Sn_{4.92}Bi_{2.54}Se_9$ with Estimated Standard Deviations in Parentheses[a]

	U_{11}	U_{22}	U_{33}	U_{23}	U_{13}	U_{12}
Bi1/Sn1′	12(1)	13(1)	16(1)	1(1)	0	0
Bi2/Sn2′	12(1)	12(1)	14(1)	1(1)	0	0
Bi3/Sn3′	10(1)	11(1)	15(1)	−1(1)	0	0
Bi4/Sn4′	13(1)	14(1)	14(1)	−1(1)	0	0
Sn1/K1′	16(2)	113(4)	34(4)	41(3)	0	0
Se1	10(1)	13(1)	13(1)	1(1)	0	0
Se2	11(1)	12(1)	9(1)	−1(1)	0	0
Se3	10(1)	9(1)	12(1)	−1(1)	0	0
Se4	10(1)	13(1)	29(1)	8(1)	0	0
Se5	21(1)	16(1)	9(1)	0	0	0

[a] The anisotropic displacement factor exponent takes the form $-2\pi^2[h^2a^{*2}U_{11} + k^2b^{*2}U_{22} + l^2c^{*2}U_{33} + 2klb^*c^*U_{23} + 2hla^*c^*U_{13} + 2hka^*b^*U_{12}]$.

Table 5. Anisotropic Displacement Parameters (10^{-3} Å^2) for $K_1Sn_5Bi_5Se_{13}$ with Estimated Standard Deviations in Parentheses[a]

	U_{11}	U_{12}	U_{13}	U_{23}	U_{13}	U_{12}
Bi1/Sn1′	17(1)	14(1)	25(1)	0	4(1)	0
Bi2/Sn2′	20(1)	17(1)	27(1)	0	3(1)	0
Bi3/Sn3′	17(1)	14(1)	21(1)	0	5(1)	0
Bi4/Sn4′	11(1)	9(1)	22(1)	0	3(1)	0
Bi5/K5′	57(1)	21(1)	174(3)	0	55(2)	0
Sn1	22(1)	22(1)	30(1)	0	6(1)	0
Se1	16(1)	17(1)	19(1)	0	4(1)	0
Se2	39(1)	14(1)	66(2)	0	37(1)	0
Se3	22(1)	20(1)	21(1)	0	1(1)	0
Se4	27(1)	36(2)	20(1)	0	5(1)	0
Se5	24(1)	22(1)	23(1)	0	2(1)	0
Se6	16(1)	16(1)	42(2)	0	−2(1)	0
Se7	17(1)	18(2)	21(2)	0	−2(1)	0

[a] The anisotropic displacement factor exponent takes the form $-2\pi^2[h^2a^{*2}U_{11} + k^2b^{*2}U_{22} + l^2c^{*2}U_{33} + 2klb^*c^*U_{23} + 2hla^*c^*U_{13} + 2hka^*b^*U_{12}]$.

Table 6. Selected Distances in Å for $K_{0.54}Sn_{4.92}Bi_{2.54}Se_9$[a]

Bi1	−Se5	2.768(1)	Bi2	−Se5	2.7264(7)	Bi3	−Se2 × 2	2.9754(7)
	−Se4 × 2	2.8995(7)		−Se1 × 2	2.8447(7)		−Se3 × 2	2.9847(7)
	−Se2 × 2	3.0431(7)		−Se4 × 2	3.1249(8)		−Se3	3.019(1)
	−Se3	3.213(1)		−Se2	3.174(1)		−Se4	3.051(1)
Bi4	−Se3 × 4	2.9756(9)	Sn1	−Sn1	0.546(5)			
	−Se2 × 2	2.9826(9)		−Se5 × 2	2.930(3)			
				−Se1 × 2	3.350(3)			
				−Se4	3.401(3)			
				−Se1 × 2	3.644(3)			
				−Se4	3.924(3)			

[a] Because of the mixed Bi/Sn occupancy on several metal sites, these distances represent only average values.

disorder of alkali metal and a heavy metal are not unusual in the systems A/Bi/Se and A/M/Bi/Se (A = K, Rb, Cs; M = Sn, Pb). Dealing with a quaternary system, we cannot exclude the possibility of a triple disorder of K, Sn, and Bi on the same crystallographic site, which is impossible to refine reliably with our X-ray data. In the known crystal structures of the A/Bi/Se and A/M/Bi/Se systems, the alkali metals prefer tricapped trigonal prismatic sites over octahedral sites. Therefore, we modeled the electron density of the Bi5 site (initially 82% Sn and 18% Bi), the only nonoctahedral site in the structure, with a mixed occupancy Bi/K disorder and a Sn/K disorder as well. The latter could not adequately represent the electron density found in this site, and the difference Fourier synthesis revealed a peak close to the Bi5 site. Consequently, we applied a mixed occupancy model with Bi and K on the Bi5 site which resulted in a 50/50 occupancy. According to this result and the charge-balanced formula $KSn_5Bi_5Se_{13}$ (with K^+, Sn^{2+}, Bi^{3+}, and Se^{2-}), we constrained the occupancies of the disordered sites. After anisotropic refinement, the R1 and wR2 values dropped to 7.5% and 14.3%, respectively. The results of the structure refinements and other crystallographic data are given in Tables 1, 3, 5, and 7.

Table 7. Selected Distances in Å for $KSn_5Bi_5Se_{13}$

Bi1	−Se3	2.804(3)	Bi2	−Se4	2.813(3)	Bi3	−Se1 × 4	2.953(2)
	−Se2 × 2	2.942(2)		−Se3 × 3	2.890(2)		−Se2 × 2	3.128(3)
	−Se1 × 2	2.975(2)		−Se2 × 2	3.034(2)			
	−Se1	3.130(3)		−Se1	3.058(3)			
Bi4	−Se4	2.805(3)	Bi5	−Se4 × 2	2.889(4)	Sn1	−Se2 × 4	2.9756(9)
	−Se5 × 2	2.872(2)		−Se3 × 2	3.274(5)		−Se1 × 2	2.9826(9)
	−Se6 × 2	3.067(2)		−Se5 × 2	3.389(5)			
	−Se7	3.068(2)		−Se2	3.538(8)			
				−Se6	3.711(8)			

[a] Because of the mixed Bi/Sn occupancy on several metal sites, these distances represent only average values.

Results and Discussion

Structure Description. The quaternary bismuth selenide $KSn_5Bi_5Se_{13}$ crystallizes in a new structure type, while $K_xSn_{6-2x}Bi_{2+x}Se_9$ adopts the structure type of the mineral heyrovskyite, $Pb_6Bi_2S_9$.[24,16c] Both fit the structural evolution of the extended lillianite series xPbS·Bi_2S_3, and are the first quaternary selenides belonging to this homologous series. In general, the arrangement of two identical slabs of the galena (or NaCl-type) lattices, as in $K_xSn_{6-2x}Bi_{2+x}Se_9$, results in the higher symmetry space group *Cmcm*, while the monoclinic space group *C*2/*m* is found for structures assembled by slabs differing in their size, as in $K_1Sn_5Bi_5Se_{15}$.

Figures 2 and 3 show a (001) projection of the structures that are both derived by tropochemical cell-twinning of NaCl-type blocks. In each case, slabs cut out of the galena lattice parallel to the (311) plane are juxtaposed in such a way that adjacent slabs are related by operations of mirrors parallel to (010), compare to Figure 1. The slabs are characterized by the number of edge-sharing octahedra running along the $(01\bar{1})$ direction of the galena lattice. Figure 4 represents the close structural relationship of $K_xSn_{6-2x}Bi_{2+x}Se_9$ and $KSn_5Bi_5Se_{13}$ by tropochemical cell-twinning. As shown in Figure 4, members of the extended lillianite series are also described by the symbol L n, n' where L indicates a member of the lillianite series and n and n' correspond to the number of octahedra in each of the two slabs involved in tropochemical cell-twinning. According to this nomenclature, we will also refer to the heyrovskyite analogue, $K_xSn_{6-2x}Bi_{2+x}Se_9$, as L 7, 7 and to $K_1Sn_5Bi_5Se_{13}$ as L 4, 5.

As seen in Figures 2 and 4, the building unit spans 7 octahedra parallel to the $(01\bar{1})$ direction of the NaCl-type lattice (indicated by an arrow in Figure 4) and three octahedra wide perpendicular to this direction in the crystal structure of $K_xSn_{6-2x}Bi_{2+x}Se_9$. While Bi3 and Bi4 in the middle of the octahedra chain show nearly ideal octahedral coordination by selenium atoms, the lone pairs of Bi^{3+} and Sn^{2+} are expressed at the periphery of the chain in a distorted octahedral environment for the Bi1 (5 + 1 coordination) and Bi2 (3 + 3 coordination) sites with interatomic distances ranging from 2.72 to 3.21 Å. All metal sites within the NaCl-type slabs are mixed occupied by Bi and Sn, where Sn prefers the center sites and Bi is accumulated at the surface of these

(24) Takeuchi, Y.; Takagi, J. *Proc. Jpn. Acad.* **1974**, *50*, 76−79.

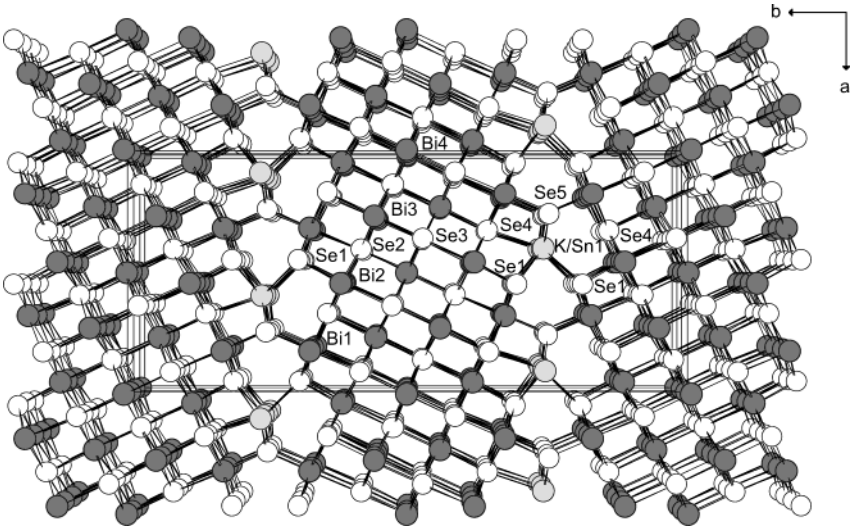

Figure 2. Projection of $K_{0.54}Sn_{4.92}Bi_{2.54}Se_9$ along the *c* axis with a slight perspective and with atom labeling.

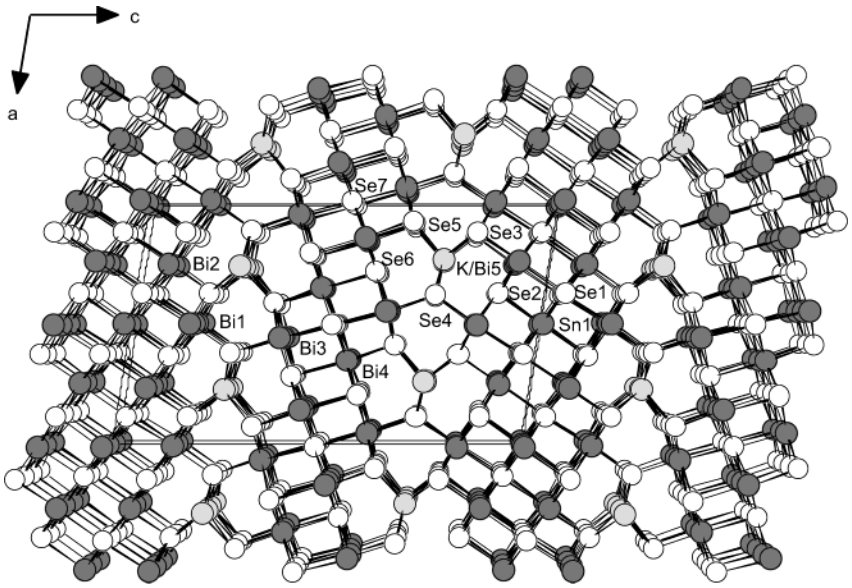

Figure 3. Projection of $KSn_5Bi_5Se_{13}$ along the *b* axis with atom labeling.

building units near the twin boundaries, see Table 2, especially in position Bi2. A similar cation contribution with Bi preferring the M2 site was also found for heyrovskyite according to valence bond calaculations[25] that agree well with the crystal structure of a Ag-bearing Bi-rich variety of heyrovskyite.[26]

The process of tropochemical cell-twinning of the NaCl-type slabs to the three-dimensional structure of $K_xSn_{6-2x}Bi_{2+x}Se_9$ generates trigonal-prismatic sites in the mirror plane that are occupied by Sn and K. The metal is shifted toward the edge of the prism that lies on the twin plane, as the strong interaction to Se5 ($d = 2.93$ Å) indicates, while the other edges are more remote with M−Se distances of 3.35 (Se1) and 3.64 (Se1) Å, respectively. If the Se4 atom ($d = 3.40$ Å) is counted, the actual coordination polyhedron for Sn1 is an monocapped trigonal prism. Another potentially capping atom Se4 lies too far (3.92) from Sn1 to be considered bonding. In comparison to heyrovskyite and its Ag bearing analogue, the coordination of the Sn1 site is more distorted due to the fact that the Sn1 site is not fixed at $z = {}^1/_4$ as in previously published structure solutions for this structure type. In addition, the mixed occupancy Sn/K will influence the coordination polyhedron of this site in comparison to an occupation by Pb and/or Bi.

In contrast to $K_xSn_{6-2x}Bi_{2+x}Se_9$, the structure of $K_1Sn_5Bi_5Se_{13}$ depicted in Figure 3 is assembled by two different building units, spanning 4 and 5 octahedra parallel to the $(01\bar{1})$ direction of the NaCl-type lattice (indicated by an arrow in Figure 4), respectively. Similar to $K_xSn_{6-2x}Bi_{2+x}Se_9$, the center position (Sn1) of the larger blocks is preferred by Sn (fully occupied by Sn), whereas Bi is accumulated on the Bi2 site at the periphery of this building unit. The 4-octahedra wide block resembles a slab found in the lillianite structure[16] (L *4,4*) where two identical building units are present. Lacking a central atomic plane, the distribution of

(25) Brown, I. D.; Altermatt, D. *Acta Crystallogr.* **1985**, *B41*, 244−247.
(26) Makovicky, E.; Mumme, W. G.; Hoskins, B. *Can. Mineral.* **1991**, *29*, 553−559.

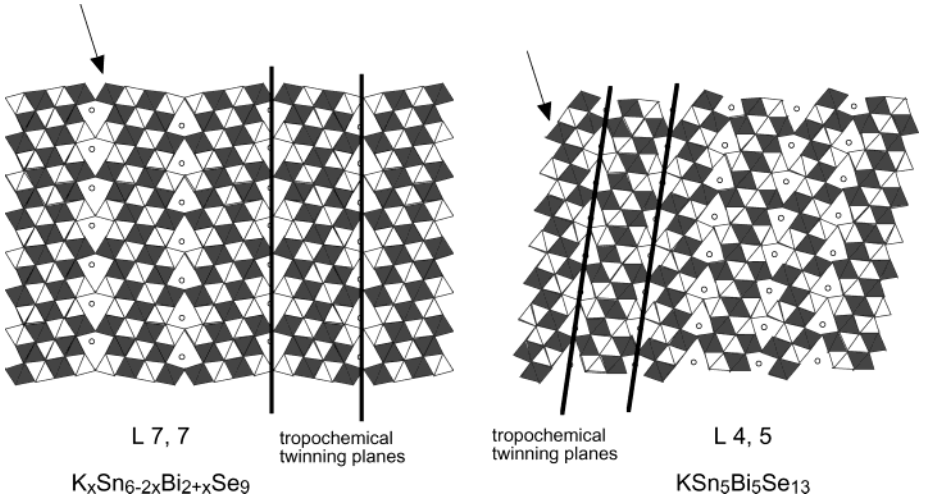

Figure 4. Comparison of $K_{0.54}Sn_{4.92}Bi_{2.54}Se_9$ and $KSn_5Bi_5Se_{13}$ (in polyhedral representation) to highlight close relationship. The structures are shown as packing of metal−selenium octahedra, those at the lower level are gray, the ones at the higher level are white. The direction of octahedra chains determining L *n*, *n*′ are indicated by arrows.

the metal atoms in this slab is more uniform with 37% Bi in the Bi3 site and 48% Bi in the Bi4 site, respectively. A similar cation distribution based on valence bond calculations was reported[25] for lillianite, $Pb_3Bi_2S_6$, with 46% Bi in the site corresponding to Bi3 and 54% Bi in the other site. Besides Sn1 with an nearly ideal octahedral coordination, the Bi1−4 sites exhibit distorted octahedral coordination with distances to Se atoms ranging from 2.8 to 3.13 Å. The bicapped trigonal-prismatic sites in the mirror plane of the tropochemical cell-twinning accommodate K and Bi in a 50/50 ratio.

Perspective and Classification of the New Quaternary Selenides. The numerous compounds discovered in the system K/Sn/Bi/Se strongly suggest that the A/M/Bi/Se system may be "infinitely adaptive".[27] In other words, small variations of the ratio of the starting materials result in new compounds with gradually evolving structural features. The mechanism of tropochemical cell-twinning is one possibility for the system to deal with small changes in the composition. The system A/M/Bi/Se seems to adjust to a new structure type each time the composition changes rather than form varying mixtures of two or more phases or form solid solutions. In the Bi rich region, we find the members of the homologous super-series $A_m[M_{1+l}Se_{2+l}]_{2m}[M_{2l+n}Se_{2+3l+n}]$ while we obtain SnSe and an unknown molecular compound from Sn rich ratios.[13] If the ratio of Sn and Bi is approximately 1, the system produces phases where tropochemical cell-twinning occurs. The phase $KSn_5Bi_5Se_{13}$ represents a new structure type of the extended lillianite series. According to electron microscopy studies,[17b] L *4, 5*; L *7, 8*; and L *8, 8* phases have been positively identified in the $Ag_2S-PbS-Bi_2S_3$ system, but no bulk material had been obtained.

It would be interesting to investigate if further members of this series can be prepared in the K/Sn/Bi/Se system. In contrast to the reported intergrowth[17] of the twinned phases in the $Ag_2S-PbS-Bi_2S_3$ system, we were able to prepare single crystals in the K/Sn/Bi/Se system. This particular system may provide many missing members of the extended lillianite series, as for example L *7, 8* and L *8, 8*. In general, these phases may have potential for thermoelectric applications. We expect a low thermal conductivity due to the fish-bone-like arrangement of the slabs of the NaCl-type lattice, which may be tunable by varying the thickness of the slabs.

Charge Transport Properties. Preliminary charge transport measurements of these phases were carried out. The electrical conductivity of the quaternary selenides described here was measured on polycrystalline ingots and found to be strongly influenced by the ingot preparation conditions. At room temperature, we observed high electrical conductivity of 1200 S/cm for $KSn_5Bi_5Se_{13}$ and 1000 S/cm for $K_xSn_{6-2x}Bi_{2+x}Se_9$, both quenched samples, while a slowly cooled sample of $K_xSn_{6-2x}Bi_{2+x}Se_9$ showed lower electrical conductivity of 650 S/cm. The high conductivity of quenched samples is attributed to the generation of a large number of defects in the structure, whose exact nature is not known but can be speculated to be M/Se antisite defects or Se vacancies.

The thermopower was measured between 300 and 400 K on polycrystalline aggregates of $K_xSn_{6-2x}Bi_{2+x}Se_9$ and $KSn_5Bi_5Se_{13}$. With rising temperature from 300 to 400 K, the negative Seebeck coefficient increases from −48 to −65 μV/K for $K_xSn_{6-2x}Bi_{2+x}Se_9$ (slowly cooled) and −16 to −27 μV/K for $KSn_5Bi_5Se_{13}$, respectively. Such low values are consistent with the high electrical conductivity of these samples. The negative values indicate n-type behavior with electrons as the dominant charge carriers.

Energy Gaps and Thermal Properties. The infrared absorption spectra of $K_xSn_{6-2x}Bi_{2+x}Se_9$ and $KSn_5Bi_5Se_{13}$ were recorded at room temperature in the range 0.1−0.7 eV, but the band gaps could not be determined reliably. This could be due to a great number of mid-gap states derived from various defects in the lattice (deriving mostly from the mixed

(27) (a) Anderson, J. S. *J. Chem. Soc., Dalton Trans.* **1973**, *10*, 1107−1115. (b) Swinnea, J. S.; Steinfink, H. *J. Solid State Chem.* **1982**, *41*, 114−123. (c) Mercurio, D.; Parry, B. H.; Frit, B.; Harburn, G.; Williams, R. P.; Tilley, R. J. D. *J. Solid State Chem.* **1991**, *92*, 449−459.

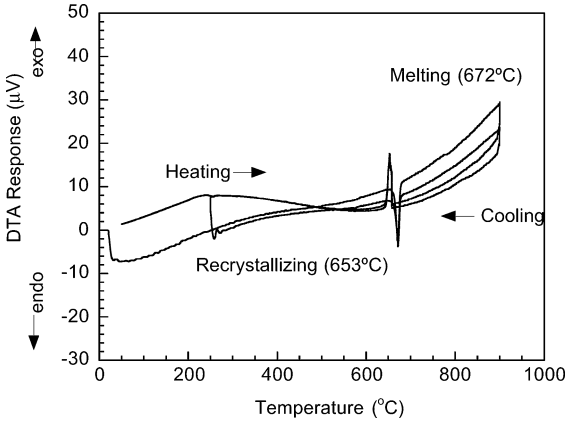

Figure 5. Differential thermogram of $KSn_5Bi_5Se_{13}$ showing melting and recrystallization events. Heating/cooling rate was 10 °C/min.

occupation of many crystallographic sites by alio-valent elements, e.g., K/Bi, Sn/Bi, or K/Sn)[28] and is consistent with the observed charge transport behavior already described.

According to DTA experiments, $K_xSn_{6-2x}Bi_{2+x}Se_9$ and $KSn_5Bi_5Se_{13}$ melt and recrystallize without structural change at 660 and 672 °C, respectively. A typical DTA diagram is shown in Figure 5 for $KSn_5Bi_5Se_{13}$. The well defined melting and crystallization events and their close proximity reflect the essentially congruent melting behavior of the material.

Concluding Remarks

The investigations in the system K/Sn/Bi/Se reported here and elsewhere[8−13] suggest that it is "infinitely adaptive". The phases $K_xSn_{6-2x}Bi_{2+x}Se_9$ and $KSn_5Bi_5Se_{13}$ reveal a new understanding for how the quaternary system K/Sn/Bi/Se adjusts to small changes in the composition. The crystal structures of both compounds showing similar structural features are derived from NaCl-type blocks by tropochemical cell-twinning of slabs cut out perpendicular to the (311) direction. The quaternary selenides belong to the extended lillianite series and are characterized by the number of metal octahedra running parallel to the $(01\bar{1})$ direction of the NaCl-type lattice. While in $K_xSn_{6-2x}Bi_{2+x}Se_9$ (L *7, 7*), two identical building units form the three-dimensional structure, $KSn_5Bi_5Se_{13}$ (L *4, 5*) features two distinct slabs. The selenides are n-type narrow band gap degenerate semiconductors with high electrical conductivity and low thermopower. The pursuit of new members of the extended lillianite series in the K/Sn/Bi/Se system is currently under way.

Acknowledgment. Financial support from the Office of Naval Research (Contract N00014-02-1-0867) and the Deutsche Forschungsgemeinschaft is gratefully acknowledged. This work made use of the SEM facilities of the Center for Advanced Microscopy at Michigan State University. Part of this work was completed by M.G.K. in Germany (Westfälische Wilhelm-Universität Münster) during an extended stay under the auspices of a Humboldt Senior Award.

Supporting Information Available: X-ray crystallographic data for $K_{0.54}Sn_{4.92}Bi_{2.54}Se_9$ and $K_1Sn_5Bi_5Se_{13}$ in CIF format. This material is available free of charge via the Internet at http://pubs.acs.org.

IC034252N

(28) Bilc, D.; Mahanti, S. D.; Larson, P.; Kanatzidis, M. G. *Phys. Rev. B*, submitted.